

# Investigation of the Electronic Properties of Organic Light-Emitting Devices by Impedance Spectroscopy

Christoph Jonda\* and Andrea B. R. Mayer

Corporate Research and Development, Robert Bosch GmbH, D-70839 Gerlingen, Germany

Received February 25, 1999. Revised Manuscript Received June 10, 1999

A key for the understanding of the electronic properties of organic light-emitting devices (OLEDs) is the frequency dependent investigation of their complex resistance. We report impedance spectroscopy measurements of electroluminescent (EL) single-layer and double-layer systems. It is shown that there are important differences found in the corresponding equivalent electrical circuits. In EL single-layer devices the electrical field decreases homogeneously over the entire layer thickness, resulting in an equivalent circuit of one RC component. In contrast, for the EL two-layer devices two RC components are necessary for the description. In both systems no indications of an insulating layer or a depletion region are found. During the measurements of the impedances of operated EL single-layer and EL two-layer systems, both under inert gas and in air, an increase of the resistance is observed. However, there are no signs for an insulating layer covering the entire contact area, through which the transport of charge carriers has to occur.

## 1. Introduction

Research efforts on organic light emitting devices (OLEDs) are increasing since these systems can offer options and advantages of high commercial interest in the field of display technology. Due to the use of organic materials it is possible, for instance, to employ well-established and low-cost deposition methods, which allow the fabrication of large-area displays and back-lighting systems. Further advantages arise from the independence of the viewing angle, the accessibility of a broad range of colors, and the option to operate these devices at dc voltages below 5 V.

Usually, OLEDs consist of an organic single-layer or multilayer system sandwiched between two electrodes, one of which has to be transparent to allow the emission of light. Indium tin oxide (ITO) is typically employed as the transparent anode material, whereas the cathode consists of a low-work function metal or metal alloy.

It has already been reported that high luminances<sup>1</sup> and efficiencies<sup>2</sup> can be obtained that are satisfactory for technological applications. Among the main obstacles still remain the insufficient lifetime and the necessity for encapsulation of these devices. Furthermore, during operation the electroluminescent intensity and the efficiency decrease, in addition to the appearance of nonemitting areas ("dark spots") accompanied by the increase of the resistance of the devices.<sup>3,4</sup>

The results obtained by impedance spectroscopy are an important basis for the detailed description and interpretation of the electrical properties of the systems. From the information gained by impedance spectroscopy, equivalent circuits for EL single-layer and EL two-layer systems can be devised. In addition, important conclusions on the distribution of the field strength within a sample can be drawn.

The goal of the impedance spectroscopical investigations was to find the qualitative differences between the EL single-layer and the EL two-layer systems with respect to their equivalent circuit and the distribution of the field strength. Furthermore, in this work impedance spectroscopical investigations were performed for several OLEDs in order to clarify to what extent possible oxide intermediate layers influence the course of the electrical field strength.

For the EL single-layer systems, only one organic layer is deposited, which also includes the electron-transporting and emitting molecules, besides the matrix polymer and the hole-transporting materials. For the EL two-layer systems a second separate layer is deposited onto the hole-transporting layer. This second layer possesses both electron-transporting and emitting properties. Since this design does not change the composition of the hole-transporting layer, an option is given to systematically compare the effects of the respective hole-transporting systems on the electrical properties and the electroluminescence behavior of the OLEDs.

Usually, a parallel connection of a resistor (R) and a capacitor (C) or, if necessary, a series connection of several of such RC components is employed as a total equivalent circuit for OLEDs.<sup>5–7</sup> The resistance de-

\* Corresponding author. E-mail: ch.jonda@t-online.de.

(1) Wakimoto, T.; Kawami, S.; Nagayama, K.; Yonemoto, Y.; Murayama, R.; Funaki, J.; Sato, H.; Nakada, H.; Imai, K. *International Symposium of Inorganic and Organic Electroluminescence*, Hamamatsu, Japan, 1994.

(2) Sano, Y.; Hamada, Y.; Shibata, K. In *Inorganic and Organic Electroluminescence/EL 96 Berlin*; Mauch, R. H., Gumlich, H.-E., Eds., Wissenschaft und Technik Verlag Dr. Jürgen Gross: Berlin, 1996.

(3) Sato, Y.; Kanai, H. *Mol. Cryst. Liq. Cryst.* **1994**, *253*, 143.

(4) Scott, J. C.; Kaufmann, J. H.; Brock, P. J.; Di Pietro, R.; Salem, J.; Goitia, J. A. *J. Appl. Phys.* **1996**, *79*(5), 2745.

(5) Karg, S. Ph.D. Thesis, University of Bayreuth, 1994.

(6) Lmimouni, K.; Tharaud, O.; Legrand, C.; Chapoton A. *L'Onde Électrique* **1994**, *74* (6), 12.

(7) Esteghamatian, M.; Xu, G. *Synth. Met.* **1995**, *75*, 149.

scribes the conductance of the layer, and the capacity reflects the layer thickness and the displacement current through the layer.<sup>8</sup> If the real and imaginary part are plotted in the complex plane, the impedance spectrum consists of the ideal case of one or several semicircles, whose diameters correspond to the respective resistances. The capacitance ( $C$ ) can be calculated from the frequencies belonging to the respective zenith according to  $C = 1/2\pi fR$  (with  $f$  = frequency,  $R$  = resistance). From the capacitance the layer thickness ( $d$ ) can be estimated according to  $C = \epsilon_0\epsilon_r A/d$  (with  $A$  = contact area,  $\epsilon_0$  = electric field constant,  $\epsilon_r$  = relative dielectric constant).<sup>9</sup>

Additional impedance spectroscopical measurements were performed after operation of the OLEDs. This can clarify how the complex resistance is changed by the current flow, and whether and to what extent any changes in the equivalent circuit, such as additional RC components, will result.

## 2. Experimental Section

**2.1. Materials.** The glass substrates coated with ITO of about 100 nm thickness were obtained from Balzers. Poly(vinylcarbazole) (PVK) was used as the matrix polymer and was purchased from Aldrich. For some experiments polystyrene (PS) or polycarbonate (PC) was employed as the matrix polymer. 1,3,5-tris[4-(di-4-methoxyphenylamino)phenyl]benzene (TDAPB-1, supplied by Bayer) or 1,3,5-tris[4-(di-4-ethylphenylamino)phenyl]benzene (TDAPB-4, supplied by Bayer) were employed as the hole-transporting materials. Aluminum tris(8-hydroxyquinoline) ( $\text{Alq}_3$ ) was synthesized by the reaction of aluminum trichloride ( $\text{AlCl}_3$ , Merck) with 8-hydroxyquinoline (Merck).

**2.2. Device Fabrication.** The ITO substrates were thoroughly cleaned by a detergent solution and deionized water, in combination with ultrasonification in the respective baths and a plasma-etching treatment prior to use. For the EL two-layer systems the polymeric, hole-transporting blend systems were deposited under nitrogen by spin coating from a filtered 1 wt % solution of PVK + TDAPB-1 or PVK + TDAPB-4 (mass ratio 1:1) in 1,2-dichloroethane. The monomeric  $\text{Alq}_3$  was vacuum deposited by thermal evaporation in a vacuum below  $10^{-5}$  mbar. Typically, the deposition rate was between 0.1 and 0.5 nm/s. For the EL single-layer systems a blend of PVK + TDAPB-1 +  $\text{Alq}_3$  or PVK + TDAPB-4 +  $\text{Alq}_3$  (mass ratio 4:1:1) was deposited under nitrogen by spin coating from a filtered 1 wt % solution in dichloroethane. For several further experiments PS or PC was employed instead of PVK as the matrix polymer. The magnesium–silver cathode (Mg:Ag = 10:1 atom %) was vapor deposited in a vacuum below  $5 \times 10^{-5}$  mbar at room temperature by simultaneous codeposition from two separate sources.

**2.3. Physical Measurements Impedance Spectroscopy.** The frequency-dependent investigation of the complex alternating-current resistance allows the description of the OLEDs by an equivalent circuit, which allows the conversion of the measured magnitudes (real and imaginary part of the impedance) into other magnitudes. A parallel connection of a capacitor and a resistance was employed as an equivalent circuit (resulting experimental magnitudes: capacitance  $C$ , resistance  $R$ ). For the impedance spectroscopical investigations a programmable impedance analyzer (Hewlett-Packard, HP 4284A) was used. This instrument supplies a frequency range from 20 Hz to 1 MHz and offers the possibility to superimpose direct voltages of  $\pm 40$  V to the signal of the alternating voltage.

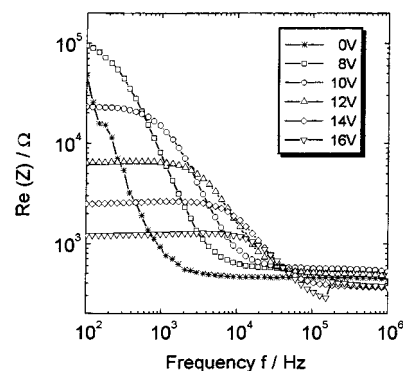


**Figure 1.** Real part of the impedance  $\text{Re}(Z)$  of an EL single-layer system (PVK + TDAPB-4 +  $\text{Alq}_3$  (4:1:1)) as a function of the frequency  $f$  at different voltages.

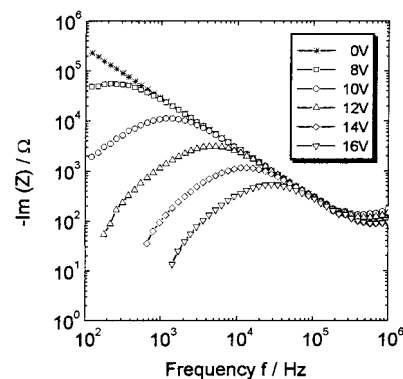


**Figure 2.** Imaginary part of the impedance  $\text{Im}(Z)$  of an EL single-layer system (PVK + TDAPB-4 +  $\text{Alq}_3$  (4:1:1)) as a function of the frequency  $f$  at different voltages.

All impedance measurements of this work were performed at room temperature and in air. The ac signal was 0.1 V for all measurements. Between 100 Hz and 1 MHz, 10 measurement values were recorded per frequency decade.

## 3. Results and Discussion

**3.1. EL Single-Layer Systems.** The goal of the impedance spectroscopical investigations with EL single-layer systems was to additionally elucidate the differences with regard to the spectra of EL two-layer systems. Some typical characteristics of the impedance spectra of single-layer systems are described below for the example ITO/PVK + TDAPB-4 +  $\text{Alq}_3$  (4:1:1)/Mg:Ag (10:1).

The real part of the impedance,  $\text{Re}(Z)$ , of an EL single-layer system as a function of the frequency  $f$  is shown in Figure 1. For voltages  $\geq 10$  V and small frequencies, the real part is almost independent of the frequency. With increasing voltage this region expands toward larger frequencies. At  $U < 10$  V such a region could not be detected, due to the limited measurement range. Adjoining this plateau the  $\text{Re}(Z)$  values strongly decrease, with the decrease occurring at higher frequencies for increasing voltages. This is followed by a second frequency-independent and only weakly voltage-dependent spectral range. Starting from  $\sim 5 \times 10^4$  Hz the course of all experimental curves is almost identical.

With increasing frequency the value of the imaginary part,  $\text{Im}(Z)$  (Figure 2), first increases, passes through a maximum, subsequently decreases again, and reaches a minimum at high frequencies ( $> 3 \times 10^5$  Hz). At 0 V

(8) Harrison, M. G.; Grüner, J.; Spencer, G. C. W. *Synth. Met.* **1996**, *76*, 71.

(9) Bellucci, F.; Valentino, M.; Monetta, T.; Nicodemo, L.; Kenny, J.; Nocilais, L.; Mijovic, J. *J. Polym. Sci., Part B: Polym. Phys.* **1994**, *32*, 2519.

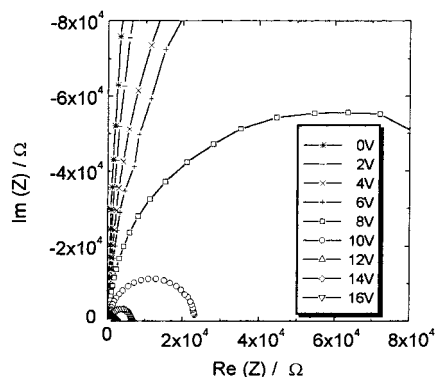


**Figure 3.** Real and imaginary part of the impedance in the complex plane (Cole–Cole plot) of an EL single-layer system (PVK + TDAPB-4 + Alq<sub>3</sub> (4:1:1)) as a function of the frequency  $f$  at different voltages.

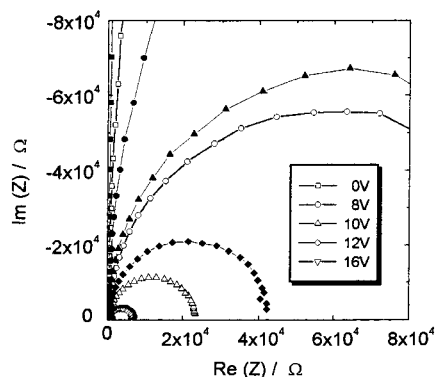


**Figure 4.** Real and imaginary part of the impedance in the complex plane (Cole–Cole plot) of an EL single-layer system (ITO/PVK + TDAPB-1 + Alq<sub>3</sub> (4:1:1)/Mg:Ag (10:1)) with different layer thicknesses at different voltages. The same symbol denotes the same voltage, the open symbols denote the smaller thickness (110 nm), and the solid symbols the larger (150 nm).

the maximum cannot be resolved, and the value of the maximum decreases with increasing voltage. Also, with increasing voltage the positions of the maxima shift to higher frequencies. In the region of about  $10^5$  Hz the course of all experimental curves is identical. In this double-logarithmic plot the positions and values of the minima show only a weak dependence on the voltage and the frequency. For the  $\text{Im}(Z)/\text{Re}(Z)$  plot (Cole–Cole plot, shown in Figure 3) semicircles result, whose diameters and positions of the zenith decrease with increasing voltage. In the spectra of EL single-layer systems only one single semicircle is found.

For the description of EL single-layer systems by an equivalent circuit, probably one single RC component is sufficient. This assumption is supported by the occurrence of one single structure resembling relaxation in the  $\text{Re}(Z)/f$  and  $\text{Im}(Z)/f$  spectra and by the existence of one single semicircle in the Cole–Cole plots. The resulting equivalent circuit as well as the resulting distribution of the field strength are discussed in detail as follows for an example incorporating TDAPB-1 as the hole-transporting component.

Figure 4 shows the real and imaginary parts in the complex plane for two samples of an EL single-layer system (ITO/PVK + TDAPB-1 + Alq<sub>3</sub> (4:1:1)/Mg:Ag (10:1)) with different layer thicknesses dependent on the applied voltage. The open symbols denote the smaller

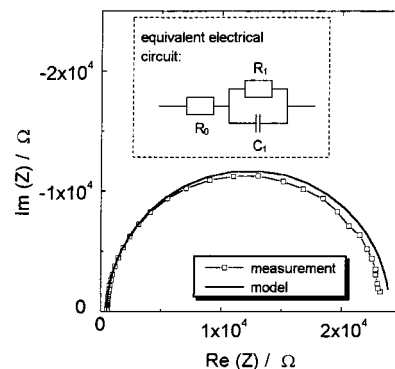


**Figure 5.** Comparison of an experimental curve from Figure 7 ( $d = 110$  nm, 10 V) with the course of the curve according to the model shown in the inset. The values for the resistances  $R_0 = 500 \Omega$  and  $R_1 = 23.5 \text{ k}\Omega$ , as well as the capacitance value  $C_1 = 5.5 \text{ nF}$ , were determined from the experimental curve.

organic layer thickness (110 nm), the solid symbols the larger (150 nm) thickness, and the same symbol shapes denote the same voltages, respectively. The frequency region lies between 100 Hz and 1 MHz. In both cases the  $\text{Re}(Z)$  and  $\text{Im}(Z)$  values initially decrease only to a small extent with increasing voltage. Only at a voltage for which also electroluminescence is observed (110 nm sample, 8 V; 150 nm sample, 10 V) the diameters of the semicircles strongly decrease. The frequency-dependent measurements of the capacitance between  $-5$  and  $15$  V, as well as the calculation of the capacitance (obtained from the zeniths of the  $\text{Im}(Z)/\text{Re}(Z)$  diagrams) result in agreeing values, namely  $6.0 \pm 0.5 \text{ nF}$  for the 110 nm sample and  $4.0 \pm 0.5 \text{ nF}$  for the 150 nm sample. A voltage dependence cannot be found. From the layer thicknesses determined by the profilometer (Tencor P-10) (110 or 150 nm) the relative dielectric constant  $\epsilon_r = 3$  is calculated according to  $\epsilon_r = Cd/\epsilon_0 A$ . This value correlates well with the data found in the literature, for instance,  $\epsilon_r(\text{OPP}) = 3.0$  (OPP = dialkoxy-substituted poly(*p*-phenylenevinylene)),<sup>10</sup>  $\epsilon_r(\text{PS/MSA}(4:1)) = 2.5$  (PS, polystyrene; MSA, tris(4-methoxystilbene)amine),<sup>11</sup> and  $\epsilon_r(\text{Alq}_3) = 4$ .<sup>12</sup>

Both samples can be described by a single semicircle; therefore, for the analogous equivalent circuit, one single RC component with a resistance  $R$  and a constant capacitance  $C$  is sufficient. Since the semicircles do not intercept the  $\text{Re}(Z)$ -axis at the origin, a resistance caused by the experimental setup ( $R_0$ ) still has to be connected in series.  $R_0$  summarizes the influences of the electrodes and of the contacts between the electrodes and the electric circuit. Figure 5 compares the course of the curve which results from this simple model (inset in Figure 5), with the measurement from Figure 7 ( $d = 110$  nm, 10 V). The employed values  $R_0 = 500 \Omega$ ,  $R_1 = 23.5 \text{ k}\Omega$ , and  $C_1 = 5.5 \text{ nF}$  were determined from the experimental curve. In the region of high frequencies (small real part) a very good agreement between the experimental curve and the model is achieved. The deviations at small frequencies could be caused by the

(10) Rikken, G. L. J. A.; Kessener, Y. A. R. R.; Braun, D.; Staring, E. G. J.; Demandt, R. *Synth. Met.* **1994**, *7*, 115.

(11) Vestweber, H.; Pommerehne, J.; Sander, R.; Mahrt, R. F.; Greiner, A.; Heitz, W.; Bässler, H. *Synth. Met.* **1995**, *68*, 263.

(12) Kalinowski, J.; Di Marco, P.; Camaioni, N.; Fattori, V.; Stampo, W.; Duff, J. *Synth. Met.* **1996**, *76*, 77.

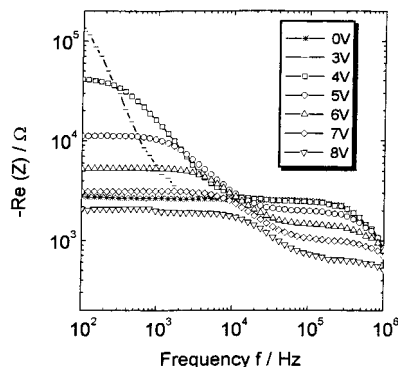


**Figure 6.** Real part of the impedance  $\text{Re}(Z)$  of an EL two-layer system (PVK + TDAPB-4 (1:1)/Alq<sub>3</sub>) as a function of the frequency  $f$  at different voltages.

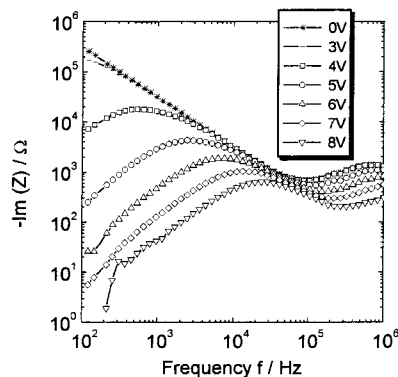


**Figure 7.** Imaginary part of the impedance  $\text{Im}(Z)$  of an EL two-layer system (PVK + TDAPB-4 (1:1)/Alq<sub>3</sub>) as a function of the frequency  $f$  at different voltages.

frequency dependence of the relative dielectric constant and of the charge carrier mobility.<sup>5</sup>

The measurements were performed in air using a Mg:Ag (10:1) contact which is sensitive to corrosion. Therefore, the existence of a thin insulating oxide layer, through which the transport of charge carriers has to occur, cannot be excluded. As a consequence, the Cole–Cole plot could have been explained also in such a way; i.e., the field strength largely decreases over the oxide layer, and the remaining bulk resistance is too small to be detected. In this case, however, no change of the dependence of resistance on the layer thickness should have been found (Figure 4), or for the sample with the larger layer thickness, a second semicircle for the larger bulk resistance should have been at least indicated. The dependence on the layer thickness of the impedance spectra shows that the electric field decreases homogeneously over the entire organic layer. No sign for a depletion region or an insulating layer can be found. These measurements and their interpretation correspond well to investigations for the system ITO/MEH-PPV/Al (MEH-PPV, poly(2-methoxy-5-(2-ethylhexyloxy)-1,4-phenylenevinylene)) already described in the literature.<sup>8</sup>

Additional comparative measurements for further EL single-layer systems were performed (with Alq<sub>3</sub> and Mg:Ag (10:1) cathodes, respectively) in order to confirm these results. With the variation of the hole-transporting molecule (TDAPB-4 instead of TDAPB-1), no change in the spectra could be observed. The influence of the matrix polymer (PS or PC instead of PVK) for the two hole-transporting materials on the experimental curves

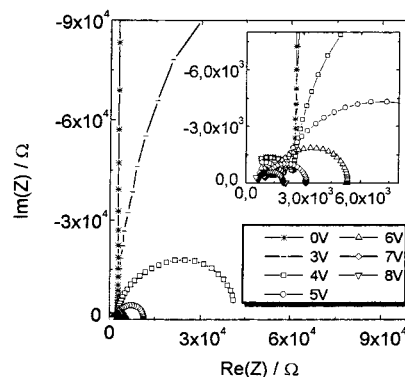


**Figure 8.** Real and imaginary part of the impedance in the complex plane (Cole–Cole plot) of an EL two-layer system (PVK + TDAPB-4 (1:1)/Alq<sub>3</sub>) as a function of the frequency  $f$  at different voltages.

was similarly small. Therefore, it can be assumed that the results discussed above for the example of the system PVK + TDAPB-1 + Alq<sub>3</sub> (4:1:1) are transferable to further EL single-layer systems incorporating Mg:Ag (10:1) contacts.

**3.2. EL Two-Layer Systems.** Several characteristics for the impedance spectra of electroluminescent two-layer systems are shown as follows for the example ITO/PVK + TDAPB-4 (1:1)/Alq<sub>3</sub>/Mg:Ag (10:1).

Figure 6 shows the real part  $\text{Re}(Z)$  of this EL two-layer system in a double-logarithmic plot as a function of the frequency  $f$  at different voltages. In the region of low frequencies the spectra typically show a frequency-independent behavior for voltages  $\geq 4$  V. Possibly this behavior also occurs for voltages  $< 4$  V at frequencies  $< 100$  Hz. This frequency region, however, was not accessible with the employed instrument. With increasing voltages this plateau extends to larger frequencies (4 V,  $10^2$  Hz  $\rightarrow$  8 V,  $10^4$  Hz), with the value of  $\text{Re}(Z)$  decreasing for more than one magnitude (4 V,  $4 \times 10^4 \Omega \rightarrow$  8 V,  $2 \times 10^3 \Omega$ , for 100 Hz, respectively). A region adjoins, where the real part decreases with increasing frequency, before a second plateau is reached. The frequency of the transition into the second frequency-independent region shifts from  $\sim 5 \times 10^3$  Hz at 3 V to  $\sim 2 \times 10^5$  Hz at 8 V, and the value of the real part in this region is smaller for higher voltages. Between  $2 \times 10^5$  and  $5 \times 10^5$  Hz again a decrease of the  $\text{Re}(Z)$  values occurs.

The imaginary part  $\text{Im}(Z)$  (see Figure 7) also turns out to be strongly dependent on the voltage and shows an undulating behavior in this double-logarithmic plot. Starting from small frequencies the imaginary part first increases and reaches a maximum, subsequently decreases, passes through a minimum, and then decreases again after a second increase at high frequencies. With increasing voltage both the maximum and the minimum (even though less clear in this double-logarithmic plot) shift to higher frequencies, and the respective  $\text{Im}(Z)$  values decrease. Because of the limited measurement range the first maximum could only be detected starting from 4 V, and the second one only up to 5 V.

A more clear hint for a possible equivalent circuit in the form of a parallel connection of a capacitor and a resistor results from the plot of the real and imaginary parts in the complex plane (Cole–Cole plot, shown in Figure 8). Here the frequency  $f$  is contained as an

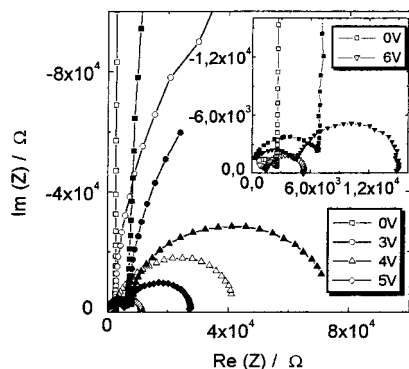


**Figure 9.** Real and imaginary part of the impedance in the complex plane (Cole–Cole plot) at different voltages for two EL two-layer systems (ITO/PVK + TDAPB-1 (1:1)/Alq<sub>3</sub>/Mg:Ag (10:1)) with hole-transporting blend systems of different thickness. The same symbol denotes the same voltage, the open symbols denote the smaller thickness (70 nm), and the solid symbols denote the larger thickness (100 nm) of the hole-transporting blend system. The layer thickness of the Alq<sub>3</sub> layer is 50 nm, respectively.

implicit variable and increases from the right (100 Hz) to the left (1 MHz). In contrast to the single-layer devices, for the two-layer systems two semicircles appear. For clarification, the small semicircle is shown enlarged in the inset.

For both the  $\text{Re}(Z)/f$  and the  $\text{Im}(Z)/f$  spectra of this EL two-layer system two structures resembling relaxation are found for voltages  $\geq 4$  V. In addition, the  $\text{Im}(Z)/\text{Re}(Z)$  plots show two semicircles. These results show that for the description of this system at least two RC components are necessary. A more detailed discussion of the equivalent circuit and the resulting distribution of the field strength follows for further examples incorporating TDAPB-1 in the hole-conducting blend system.

In Figure 9 the real and imaginary parts in the complex plane for two EL two-layer systems (ITO/PVK + TDAPB-1 (1:1)/Alq<sub>3</sub>/Mg:Ag (10:1)) are shown. The samples only differ in the layer thickness of the hole-transporting blend system (70 and 100 nm). The same symbol shapes denote the same voltages, and open symbols denote the smaller thickness, while the solid symbols denote the larger one. The frequency as implicit variable increases from the right to the left from 100 Hz to 1 MHz. In comparison to the EL single-layer systems, a second, additional semicircle appears for small  $\text{Re}(Z)$  values, whose diameter increases with the layer thickness of the hole-transporting blend system (see the inset of Figure 9). As soon as electroluminescence is observed both semicircles show a strong voltage dependence. Starting from  $U \geq 5$  V the ratio of both diameters is about 1:2.5. From this value the distribution of the field strength can be estimated. The capacitances of the samples at  $U = 0$  V are 6 nF for 70 nm and 5 nF for the 100 nm layer thickness of the hole-transporting blend system. With increasing voltage both values decrease continuously to 5 and 4 nF, respectively, at  $U = 8$  V.

For the EL single-layer systems with Mg:Ag (10:1) as the cathode material the existence of an insulating layer could not be shown. This result is most probably transferable to the EL two-layer systems, since the same materials and identical measurement conditions

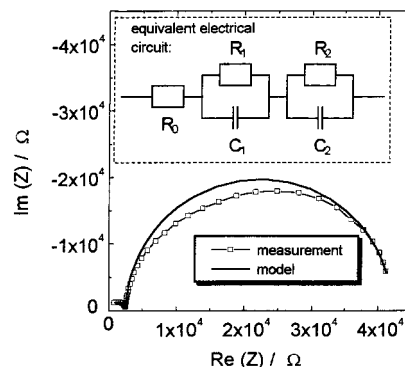


**Figure 10.** Comparison of an experimental curve from Figure 9 (shown ( $d_{\text{hole-transporting blend system}} = 70$  nm,  $U = 4$  V) with the course of the curve according to the model shown in the inset. The values  $R_0 = 100$   $\Omega$ ,  $R_1 = 2.5$  k $\Omega$ ,  $C_1 = 0.08$  nF,  $R_2 = 39.5$  k $\Omega$ , and  $C_2 = 6.0$  nF were determined from the experimental curve.

were employed. Therefore, the small semicircle in Figure 9 can be assigned to the hole-transporting blend system ( $R_1$ ,  $C_1$ ), and the larger semicircle is due to the Alq<sub>3</sub> layer ( $R_2$ ,  $C_2$ ). The differences in diameter can be explained by the probably much smaller conductivity of the Alq<sub>3</sub> layer.<sup>13,14</sup> In comparison to the EL single-layer systems, the equivalent circuit for an EL two-layer system has to be extended by a second RC component with possible resistances caused by the experimental setup or contact resistances  $R_0$  being taken into consideration. Figure 10 shows both the equivalent circuit and the resulting course of the curve. The employed  $R$  and  $C$  values ( $R_0 = 100$   $\Omega$ ,  $R_1 = 2.5$  k $\Omega$ ,  $C_1 = 0.08$  nF,  $R_2 = 39.5$  k $\Omega$ ,  $C_2 = 6.0$  nF) were determined from the experimental curve in Figure 9, which is shown as well ( $d_{\text{hole-transporting blend system}} = 70$  nm,  $U = 4$  V). With these values a very good agreement is obtained for frequencies  $f < 300$  Hz, starting from  $f > 5$  kHz. Only in the regions between these two frequencies the experimental curve is more flat due to the frequency dependence of  $\epsilon_r$  and of  $\mu_{n,p}$  ( $\mu_n$  = electron mobility,  $\mu_p$  = hole mobility).

To our knowledge, impedance spectroscopical investigations for EL two-layer systems could not be found in the literature. However, similar spectra containing two semicircles were measured for ITO/PPV/Al diodes (PPV = poly(*p*-phenylenevinylene)).<sup>8,15</sup> In this case the small semicircle at high frequencies is interpreted as bulk resistance, whereas the large semicircle at low frequencies is caused by the depletion region of the Schottky contact. Especially the large semicircle turns out to be strongly dependent on the voltage. At higher voltages, however, and as soon as electroluminescence occurs, it cannot be resolved anymore, due to the disappearance of the depletion region. Within a certain voltage range the PPV systems thus can also be regarded as “two-layer systems” (bulk and depletion region). This interpretation, however, cannot be applied for the organic LEDs investigated in this work, because neither any signs for the existence of a Schottky contact

(13) Nakamura, H.; Hosokama, C.; Kusumoto, T. In *Inorganic and Organic Electroluminescence/EL 96 Berlin*; Mauch, R. H., Gumlich, H.-E., Eds.; Wissenschaft und Technik Verlag Dr. Jürgen Gross: Berlin, 1996.

(14) Hosokawa, C.; Tokailin, H.; Higashi, H.; Kusumoto, T. *Appl. Phys. Lett.* **1992**, *60* (10), 1220.

(15) Karg, S.; Riess, W.; Dyakonov, V.; Schwoerer, M. *Synth. Met.* **1993**, *54*, 427.

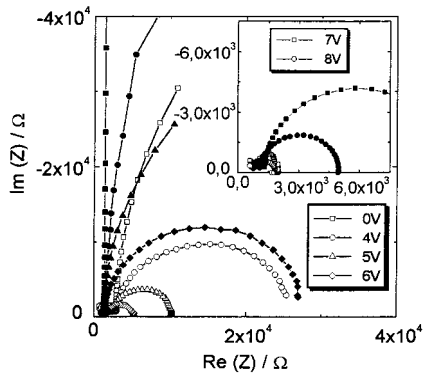


**Figure 11.** Voltage dependence of the real and imaginary part of the impedance (Cole–Cole plot) of an EL two-layer system (PVK + TDAPB-1 (1:1)/Alq<sub>3</sub>) before and after operation (18 h,  $j_{\text{const}} = 8 \text{ mA/cm}^2$ ). The same symbol shapes correspond to the same voltages, the open symbols denote the nonoperated contact, and the solid symbols the operated contact.

(insufficient diode behavior with rectification ratios of  $10^2$ – $10^3$ , too small dependence of the capacitance on the voltage) are present nor the blending together of the two semicircles in the impedance spectra is observed.

The explanations discussed in this section were confirmed by further measurements for EL two-layer systems with different hole-transporting blend systems (TDAPB-1 in a PS or PC matrix, and TDAPB-4 in a PVK, PS, and PC matrix; mass ratio 1:1, respectively). The results show that the assumptions with respect to the distribution of the field strength and the equivalent circuit can be applied to further EL two-layer systems incorporating this design.

**3.3. Impedance Spectroscopy of Samples after Operation.** The investigation of the impedance of samples after operation can clarify how the complex resistance is altered by the current flow and whether any changes in the equivalent circuit, such as additional RC components, result.

**3.3.1. EL Two-Layer Systems after Operation.** A standard EL two-layer system (PVK + TDAPB-1 (1:1)/Alq<sub>3</sub>) was operated for 18 h at a constant current density of  $8 \text{ mA/cm}^2$  in a nitrogen atmosphere. In the course of operation the voltage increased from 7.6 to 9.9 V. Figure 11 shows the dependence of the  $\text{Im}(Z)/\text{Re}(Z)$  experimental curves of the contact before (open symbols) and after operation (solid symbols) on the voltage (the same symbol shapes correspond to the same voltages). For clarity the experimental values for the higher voltages are shown in the inset. Also after operation two semicircles still appear, however, the minimum is shifted to smaller  $\text{Re}(Z)$  values. Therefore, the second, smaller semicircle in the used contact can only be resolved rudimentary. However, in analogy to the nonoperated systems two RC components suffice for the description of the equivalent circuit. In the large semicircles the increase of the complex resistance can be clearly seen, since both the diameters and the positions of the zenith reach larger values. A comparison of the experimental curves of the nonoperated contact starting from 4 V with the  $\text{Im}(Z)/\text{Re}(Z)$  curves of the operated contact, which are increased by 2 V, reflects very well the increase of the voltage which was measured during operation.

**3.3.2. EL Single-Layer Systems after Operation.** The changes in the  $\text{Im}(Z)/\text{Re}(Z)$  diagrams of an EL

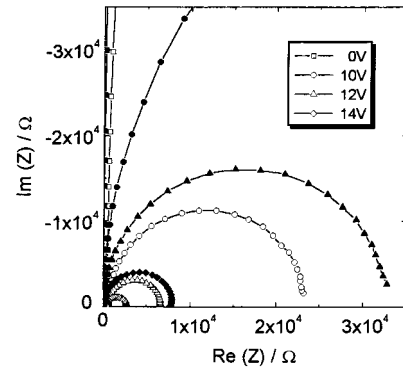


**Figure 12.** Voltage dependence of the real and imaginary part of the impedance (Cole–Cole plot) of an EL single-layer system (PVK + TDAPB-4 + Alq<sub>3</sub> (4:1:1)) before and after operation (2 h in air,  $U_{\text{const}} = 16 \text{ V}$ ). The same symbol shapes correspond to the same voltages, the open symbols denote the nonoperated contact, and the solid symbols the operated contact.

single-layer system (PVK + TDAPB-4 + Alq<sub>3</sub> (4:1:1)) after operation for 2 h in air at a constant voltage of 16 V is shown in Figure 12. Open symbols denote the nonoperated contact, solid ones the operated contact, and the same symbol shapes correspond to the same values for the voltage. Again, the shape of the experimental curve in the Cole–Cole plot did not change; merely a strong increase of the complex resistance at the same voltages is observed. This sample was operated in air in order to additionally investigate how the appearance of “dark spots” (which are formed especially fast in air) influence the impedance spectra. One assumption was that parts of the magnesium–silver contact oxidize, and a thin insulating layer is formed in these areas of the interface organic layer/cathode, which appear as dark spots. As a consequence, an inhomogeneous distribution of the field strength would result in these oxidized areas, where the electric field mainly decreases over the thin insulating layer at the interface and only to a small extent over the remaining organic layer. In the impedance spectra such a distribution would result in two semicircles, analogous to the spectra for the EL two-layer systems. The larger semicircle would have to be assigned to the contact and the smaller semicircle to the organic layer. The measurements show, however, that still one single RC component is sufficient for the description of the equivalent circuit.

The measured impedance spectra can be brought into agreement with the observed “dark spots”, with the assumption that initially only small regions of the contact area are oxidized. These are observed as non-emitting regions in the active area, since no injection of electrons occurs. The transport of the charge carriers still proceeds through the nonoxidized regions in the contact area. Therefore, in the Cole–Cole plots no second semicircle is observed. With the increase of the “dark spots” in the course of operation, however, the effective contact area through which the charge transport can occur is reduced, which results in a higher necessary voltage.

## 4. Conclusions

The results of the impedance spectroscopical investigations for EL single-layer and EL two-layer systems

can be summarized as follows: EL single-layer systems can be described by an equivalent circuit with one RC component and a resistance caused by the experimental setup. The field strength decreases homogeneously over the entire layer thickness. No signs for the existence of an insulating layer or a depletion region are found. For EL two-layer systems two RC components and one resistance caused by the experimental setup are necessary for the description of the equivalent circuit. The electric field decreases mainly over the vapor-deposited Alq<sub>3</sub> layer.

The measurements of the impedances of operated EL single-layer and EL two-layer systems both under inert gas and in air gave no indication of an insulating layer covering the entire contact area, through which the transport of charge carriers has to occur. The observed increase of the resistance can be explained by the thermally induced rearrangement of the molecules, such as dimerization or crystallization. These sites can act as traps for the charge carriers and lead to space charge

effects, which again hinder the injection of charge carriers.<sup>16</sup> One further mechanism which may cause the increase of the voltage is the reduction of the effective contact area through which the transport of the charge carriers can proceed, e.g., by the partial oxidation of the cathode.

**Acknowledgment.** This work was supported by the Bundesministerium für Bildung und Forschung, the Bayer AG, and the Robert Bosch GmbH. We would like to thank Dr. L. Weber, Corporate Research and Development, Robert Bosch GmbH, for preparing the Alq<sub>3</sub>. Furthermore, we are grateful to Dr. M. Hüppauff, Mr. W. Grothe, and Mrs. B. Grothe, Corporate Research and Development, Robert Bosch GmbH, for their support and sample preparation.

CM991024B

---

(16) Adachi, C.; Nagai, K.; Tamoto, N. *Appl. Phys. Lett.* **1995**, *66* (20), 2679.